Theory of Raman enhancement by two-dimensional materials: Applications for graphene-enhanced Raman spectroscopy

Theory of Raman enhancement by two-dimensional materials: Applications for graphene-enhanced Raman spectroscopy

E. B. Barros[1,2,*] and M. S. Dresselhaus[2]

[1]*Departamento de Física, Universidade Federal do Ceará, Fortaleza, Ceará, 60455-760 Brazil*
[2]*Department of Physics, Massachusetts Institute of Technology, Cambridge, Massachusetts 02139, USA*

We propose a third-order time-dependent perturbation theory approach to describe the chemical surface-enhanced Raman spectroscopy of molecules interacting with two-dimensional (2D) surfaces such as an ideal 2D metal and graphene, which are both 2D metallic monolayers. A detailed analysis is performed for all the possible scattering processes involving both electrons and holes and considering the different time orderings for the electron-photon and electron-phonon interactions. We show that for ideal 2D metals a surface enhancement of the Raman scattering is possible if the Fermi energy of the surface is near the energy of either the HOMO or the LUMO states of the molecule and that a maximum enhancement is obtained when the Fermi energy matches the energy of either the HOMO or the LUMO energies plus or minus the phonon energy. The graphene-enhanced Raman spectroscopy effect is then explained as a particular case of a 2D surface, on which the density of electronic states is not constant, but increases linearly with the energy measured from the charge neutrality point. In the case of graphene, the Raman enhancement can occur for any value of the Fermi energy between the HOMO and LUMO states of the molecule. The proposed model allows for a formal approach for calculating the Raman intensity of molecules interacting with different 2D materials.

I. INTRODUCTION

The recent observation of Raman signal enhancement for different molecules adsorbed on graphene has given rise to an important debate as to the origin of this effect, which has been generally referred to as the graphene-enhanced Raman spectroscopy effect (GERS) [1–6]. For example, Jung *et al.* attributed the enhancement of the Raman intensity of bromine and iodine ions adsorbed on graphene to a multiple reflection mechanism, which enhances both the incoming and scattered electric fields [3]. Also, Xie *et al.* reported that the luminescence quenching of R6G molecules on the surface of graphene allowed for a better observation of this molecular Raman spectrum [7]. However, as it was experimentally observed originally in 2010 by Ling *et al.* [1], the Raman intensity of phthalocyanine, rhodamine 6G, protoporphyrin IX, and crystal violet molecules all have very different enhancement factors. Furthermore, it has been shown that enhancement factors are strongly dependent on which molecule is being probed, on the laser excitation energy used, on the two-dimensional (2D) material used for the enhancement surface [8–10] and even on the Fermi energy of the system, as controlled by a gate voltage [6,11,12]. The dependence of the enhancement on all these parameters cannot be explained either in terms of multiple reflections, nor by the quenching of the luminescence, nor even by a combination of both. This interesting behavior seems to point towards a combination of these factors with a chemical coupling between the molecule and graphene, which would be strongly dependent on the relation between the molecule and the surface.

Surface-enhanced Raman spectroscopy (SERS) has been widely applied for the study of molecules [13–19]. The enhancement of the Raman intensity is usually explained as a combination of two effects, the first, and most important one, is the enhancement of the electromagnetic field by the light interaction with plasmons in the metallic surface (known as EM-SERS) [20]. The other process, with a magnitude that is usually smaller, is related to the chemical interaction between the molecule and the rough metallic surface, and is usually referred to as chemical-SERS or charge-transfer-SERS (which we will here refer to as CT-SERS) [13,21]. The first and most prominent effect is strongly based on the geometry of the surface and requires no chemical interaction between the molecule and the surface, such that, in principle, any molecule can be enhanced by any metallic surface provided that the experimental conditions for exciting the plasmon are met and provided that the molecule sits in a location where the electromagnetic field is enhanced. It is well known that in the case of molecules adsorbed on pure 2D materials, the EM-SERS effect should be negligible due to its geometry, which lacks the curvature that allows for the electromagnetic enhancement. In this sense, 2D materials are perfect systems for the investigation of the CT-SERS effect.

The most commonly used theories for modeling the CT-SERS effect are based on the approach developed by Lombardi *et at.* [13,21], which has its foundations in Albrecht's theory for vibronic coupling [22]. Albrecht's theory is deemed to be appropriate to describe systems for which the electronic and vibrational coordinates are strongly coupled, such that the excitations of the system can no longer be separated into these categories, but are instead a mix between electronic excitations and vibrations. Such is the case of isolated molecules, for which the electronic states are strongly modified by the atomic displacements associated with the vibrational states of the molecule. However, in the case of SERS, the molecules are usually weakly coupled to the surface, making it harder to justify applying the vibronic theory developed by Albrecht. Recently, an alternative model for the CT-SERS effect was proposed by Persson *et al.* based on a change of the surface

*ebarros@fisica.ufc.br

polarizability due to the vibrations of the molecule [23]. The model proposed by Persson is appropriate for explaining the SERS effect under nonresonance conditions.

Much benefit can result from the use of 2D materials for Raman enhancement. For example, for the usual surface-enhancement effect, only molecules which are positioned close to the hot spots of the electromagnetic film can be strongly enhanced [20]. The distribution of the molecule's location and orientation with respect to the enhanced electric field cannot be controlled with precision. On the other hand, 2D materials, such as graphene, boron nitride, and transition-metal dichalchogenides, are quite homogeneous. Therefore, the Raman enhancement will be approximately the same for each molecule adsorbed to the surface, thereby allowing for an easier quantitative interpretation of the experimental results and a better control of the experimental setup.

However, in order to further develop the application of 2D materials for enhancing the Raman intensity of molecules, it is necessary to improve our understanding of this effect and to establish a formal approach for modeling this Raman-enhancement effect. Furthermore, since Albrecht's theory [22] is mainly based on a semiclassical approximation, it lacks the mathematical rigor necessary for further developing our understanding of this interesting process. For example, within Lombardi's theory for the CT-SERS effect [13,21], the Fermi level dependence of the SERS effect is included, *a posteriori*, after all the electron-vibration interactions are taken into account, disregarding the possible interactions between the vibration and the holes left behind in the valence band.

In solid state physics, the Raman intensity is usually explained in terms of third-order time-dependent perturbation theory (TDPT) [24]. In this paper, we argue that, since the coupling between the electrons and vibrations in the molecule-surface system is expected to be rather weak, TDPT is a more appropriate framework to explain and model the Raman-enhancement effect in 2D materials. With this in mind, in this paper we develop a general theory for the Raman enhancement in 2D materials using a time-dependent perturbation theory in which the effect of many-body interactions is explicitly considered. In this sense, the enhancement effect is understood as a resonant Raman scattering process, involving electronic states of the 2D surface that are made available for the excitation by the molecule-surface interaction. Our aim here is to lay down the basic theoretical framework which will allow for more detailed calculations of the Raman enhancement due to the molecule-2D material interaction, as well as support the interpretation of experimental results. To exemplify the application of the theory developed here, we first analyze the resonance enhancement for a molecule interacting with an idealized 2D metal, for which the density of states is constant throughout the relevant energy range. The relative simplicity of this system allows for a deeper understanding of the enhancement process. We then analyze the GERS effect by considering graphene as a 2D metal with a density of states that increases linearly with the energy (as measured from the charge neutrality point).

This paper is organized as follows. In Sec. II, we review the theory of Raman scattering within the framework of TDPT by considering many-body electronic states for both the molecule and the surface. Then in Sec. III A, we discuss the nature of

the molecule-surface coupling and how this coupling can be expressed in terms of electron-phonon and electron-photon matrix elements. We also discuss how this information may, on one hand, guide future theoretical calculations of this effect and, on the other hand, may help with simplifying our analysis of the molecule-surface interaction. In Sec. III B, we apply the TDPT model developed in Sec. II to describe the surface-enhanced Raman scattering process in the case of a two-state molecule interacting with a general 2D surface, discussing the possible Raman scattering processes contributing to the total Raman enhancement and the conditions for which the Raman intensity can be maximized. Following, this discussion, in Sec. IV, we investigate the Raman-enhancement process for a two-state molecule interacting with an ideal 2D metal and with graphene, discussing how the difference in the density of states for the two systems affects the Raman enhancement. Finally, in Sec. V we discuss how the theory developed here can be further advanced and how it can be applied to improve our understanding of the molecule-surface interaction, which ends with a summary of this paper in Sec. VI.

II. RAMAN SCATTERING THEORY

For the description of the Raman-enhancement effect by 2D materials, we propose using the following Hamiltonian:

$$H = H_0 + H_{er} + H_{ep}, \tag{1}$$

where H_0 is the equilibrium Hamiltonian for the system, which includes a molecular (H_M) part, a surface (H_S) part, and a coupling term (H_{SM}). The coupling term is assumed here to be evaluated at the equilibrium position for both the surface atoms and the atoms within the interacting molecule. For the time being, we will not discuss whether the electronic states of the molecule and the surface are being mixed or not by the H_{SM} interaction. For now, it suffices to assume that the eigenstates of the equilibrium Hamiltonian H_0 can be described as a combination of eigenstates localized at the molecule and eigenstates localized at the surface atoms.

The remaining terms in Eq. (1), namely H_{er} and H_{ep}, correspond to the electron-radiation and electron-phonon (or electron-vibration) interactions, respectively, and are treated using perturbation theory. The electron-radiation term can be written as

$$H_{er} = \sum_{jj'\alpha} M^{er}_{jj'\alpha} C^\dagger_{j'} C_j (a^\dagger_\alpha + a_\alpha) \tag{2}$$

and the electron-phonon coupling as

$$H_{ep} = \sum_{qjj'} M^{ep,q}_{jj'} C^\dagger_{j'} C_j (b^\dagger_q + b_q), \tag{3}$$

where $C^\dagger_j$ (C_j), $b^\dagger_q$ (b_q), and $a^\dagger_\alpha$ (a_α) are creation (annihilation) operators for the electronic, vibrational (phonon), and photon states, respectively. Note that j is a shorthand notation for all relevant quantum numbers regarding the electronic state, including momentum, spin, and whether the state belongs predominantly to the molecule or to the surface. In a similar way, α is a shorthand symbol for the quantum numbers of the photon state, including momentum and polarization, and q is used to label the phonon state. Again, q can be related either to

the molecular vibrational modes or to phonon states localized in the surface, in which case q gathers information about the phonon branch and phonon wave vector.

It is now important to introduce a few considerations about the possible many-body states. First, we will assume that when the molecule is not in contact with the surface, the main spectroscopic properties of the molecule can be described in terms of its highest occupied molecular orbital (HOMO) and its lowest unoccupied molecular orbital (LUMO). Also, in the absence of molecules, the surface electronic states are described by an electronic band (or a set of electronic bands in the case of a semiconducting surface) in which the Fermi energy (E_F) is defined as the energy of the highest occupied electronic state of the surface. As we will see in the following, the relationship between the HOMO and LUMO energies of the molecule and the Fermi energy of the metal will be one of the determining factors governing the intensity of the Raman enhancement. The alignment between the energy levels of the two systems (molecule and surface) requires a common definition of the energy scale (zero energy). One possible way of obtaining valuable information about this common energy scale is by measuring the ionization potential of the molecule when interacting with the 2D material.

When the molecule is in contact with the substrate, the surface-molecule interaction can be classified in terms of two broad classes: interaction without charge transfer and with charge transfer. In the first situation, the occupancy of the HOMO and/or the LUMO states will not be modified by the interaction. This is usually the case when the HOMO state is positioned well below the Fermi level of the surface and the LUMO state is above it. In the second case (with charge transfer), the distribution of electronic states is not so trivial and the HOMO state of the molecule can become partially or totally unoccupied, or the LUMO state can be occupied by electrons coming from the surface. It is convenient to consider a general theory through which the initial many-body state I can be written as

$$|I\rangle = |111\ldots 0000\rangle, \tag{4}$$

where the 1 denotes occupied states either in the molecule or on the surface. Here, we are assuming zero temperature, for simplicity.

In this work we will focus on the Stokes Raman process, for which a phonon is created. A similar formalism can be applied for the anti-Stokes Raman process, for which the detailed processes involving phonon absorption are taken into account, but this latter process will not be shown here explicitly.

We thus define the initial state of the system as composed of a single photon with a general quantum number σ and energy $\hbar\omega_\sigma = \hbar\omega_0$, an electronic system in an initial configuration $|I\rangle$, and a number n_q of phonons with quantum number q. The final state is defined as having a scattered photon with quantum number ρ, one extra phonon with a general quantum number q ($n_q + 1$) and with the electrons returning to the initial many-body state (ground state $|I\rangle$). Energy is conserved throughout the process, such that we have $\hbar\omega_\rho = \hbar\omega_0 - \hbar\omega_q$. By the Fermi golden rule, the Raman intensity I_{Raman} will be proportional to the square of the Raman matrix element

$$I_{\mathrm{Raman}} \propto |\langle \rho, n_q+1, I | M_{\mathrm{Raman}} | \sigma, n_q, I \rangle|^2. \tag{5}$$

When evaluating the Raman scattering intensity, it is necessary to consider all possible time-ordered scattering processes. There are three possible time orderings for the electron-photon and electron-phonon interactions which will relevantly contribute to the Raman scattering intensity: (rpr) photon absorption–phonon emission–photon creation; (rrp) photon absorption–phonon emission–phonon creation; and (prr) phonon creation–photon absorption–photon emission. In most common scenarios, the resonance Raman intensity can be interpreted as arising from a single resonant transition between an occupied and an unoccupied electronic state of the system. In such cases, only the (rpr) process will be relevant for the Raman intensity, and for this reason it is unnecessary to consider the other two terms. In the case of the molecule interacting with the surface, the resonance Raman process can involve more than two different electronic states, and thus all the time-ordered processes need to be taken into account.

The scattering amplitude for each of the time sequences will be slightly different and the total scattering amplitude is given by the sum between three terms: $W_{\sigma,\rho,q} \equiv W_{\sigma,\rho,q}^{(rpr)} + W_{\sigma,\rho,q}^{(rrp)} + W_{\sigma,\rho,q}^{(prr)}$. These terms can be written as

$$W_{\sigma,\rho,q}^{(rpr)} = \sum_{ik'k} \chi_{k'k}^{iq} \frac{M_{ik'}^{er,\rho} M_{k'k}^{ep,q} M_{ki}^{er,\sigma}}{(E_{k'} - E_i + \hbar\omega_q - \hbar\omega_0)(E_k - E_i - \hbar\omega_0)}$$
$$+ \xi_{k'k}^{iq} \frac{M_{kk'}^{er,\rho} M_{ik}^{ep,q} M_{k'i}^{er,\sigma}}{(E_{k'} - E_k + \hbar\omega_q - \hbar\omega_0)(E_{k'} - E_i - \hbar\omega_0)}, \tag{6}$$

$$W_{\sigma,\rho,q}^{(rrp)} = \sum_{ik'k} \chi_{k'k}^{iq} \frac{M_{ik'}^{ep,q} M_{k'k}^{er,\rho} M_{ki}^{er,\sigma}}{(E_k - E_i - \hbar\omega_0)(E_{k'} - E_i - \hbar\omega_q)}$$
$$+ \xi_{k'k}^{iq} \frac{M_{kk'}^{ep,q} M_{ik}^{er,\rho} M_{k'i}^{er,\sigma}}{(E_{k'} - E_i - \hbar\omega_0)(E_{k'} - E_k - \hbar\omega_q)}, \tag{7}$$

$$W_{\sigma,\rho,q}^{(prr)} = \sum_{ik'k} \chi_{k'k}^{iq} \frac{M_{ik'}^{er,\rho} M_{k'k}^{er,\sigma} M_{ki}^{ep,q}}{(E_{k'} - E_i + \hbar\omega_q - \hbar\omega_0)(E_k - E_i + \hbar\omega_q)}$$
$$+ \xi_{k'k}^{iq} \frac{M_{kk'}^{er,\rho} M_{ik}^{er,\sigma} M_{k'i}^{ep,q}}{(E_{k'} - E_k + \hbar\omega_q - \hbar\omega_0)(E_{k'} - E_i + \hbar\omega_q)}. \tag{8}$$

Here, i, k', and k specify single-electron states of the system and we define the functions $\chi_{k'k}^{iq}$ and $\xi_{k'k}^{iq}$:

$$\chi_{k'k}^{iq} = \begin{cases} \sqrt{n_q+1}\, f_i(1-f_k)(1-f_{k'}), & \text{if } i \neq k \neq k' \\ \sqrt{n_q+1}\, f_i(1-f_k), & \text{if } k' = k \text{ or } i = k \text{ or } k' \end{cases} \tag{9}$$

and

$$\xi_{k'k}^{iq} = \begin{cases} \sqrt{n_q+1}\, f_i f_k(1-f_{k'}), & \text{if } i \neq k \neq k' \\ 0, & \text{if } k' = k \text{ or } k' = i \end{cases} \tag{10}$$

where f_i, $f_{k'}$, and f_k are the occupancies (1 or 0) for each of these states in the initial state $|I\rangle$.

Note that for each process there are two terms, one proportional to $\chi_{k'k}^{iq}$ and one proportional to $\xi_{k'k}^{iq}$. The first term can be interpreted in terms of electron-phonon scattering and the second in terms of hole-phonon scattering. To clarify this
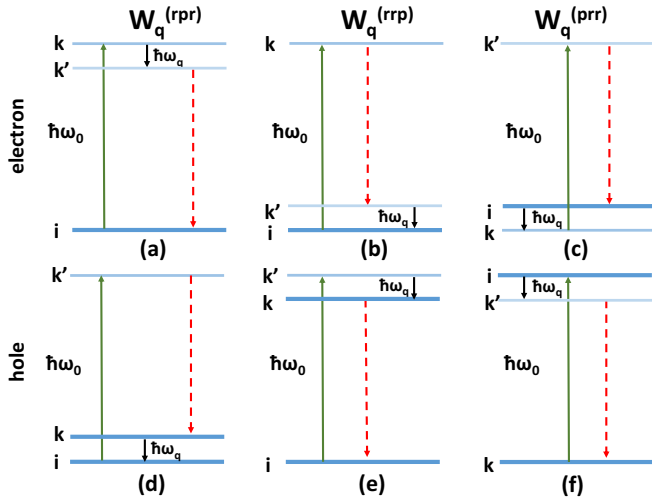
FIG. 1. (Color online) Resonance diagram for a system which is fully resonant with each of the $W_{\sigma,\rho,q}^{(rpr)}$, $W_{\sigma,\rho,q}^{(rrp)}$, and $W_{\sigma,\rho,q}^{(prr)}$ processes. Horizontal lines represent the position of the electronic states for the six possible cases. Green arrows represent the absorption of a photon with energy $\hbar\omega_0$, black arrows represent the creation of a phonon with energy $\hbar\omega_q$, while the red dashed arrows represent the emission of a photon with energy $\hbar\omega_0 - \hbar\omega_q$. The events are sequenced from left to right.

interpretation, we show in Fig. 1 the schematics for both terms in the three processes, considering fully resonance scenarios for each term, i.e., the electronic states are such that the denominator for each term can vanish. It can be seen, for example, that the (rpr)-hole process can be interpreted exactly as the (rpr)-electron process but exchanging the electron for a hole and inverting the sign of the energy and the same is true for the other processes.

III. APPLICATION TO RAMAN ENHANCEMENT BY 2D MATERIALS

The importance of each of the three processes described in the last section is defined by two factors: the magnitude of the electron-phonon and electron-radiation matrix elements and the energy balance between the molecule, for which the states are quantized with energy differences on the order of several electron volts and the surface electronic states, which can be continuous. In the following, we discuss the matrix elements governing each of these processes and we make some simplifying considerations for the case of an ideal 2D metal. We then discuss the possible resonance conditions for each process.

A. Matrix elements

1. Electron-phonon matrix elements

For the electron-phonon interaction, the matrix elements are given by

$$M_{qjj'}^{ep} = \sum_s \sqrt{\frac{\hbar}{2NM_s\omega_q}}\, \vec{e}_{qs} \cdot \int d^3r\, \psi_{j'}^*(\vec{r})\psi_j(\vec{r})\vec{\nabla}_s U(\vec{r})e^{i\vec{Q}_q\cdot\vec{r}},$$

(11)

where N is the number of atoms in the system, M_s is mass of the atom s, $\vec{Q}_q$ is the phonon wave vector, ω_q is the phonon frequency, and $\vec{e}_{qs}$ represents the unit movement of atom s for the vibrational mode defined by the quantum number q. Again, we are, in principle, assuming that both j and q represent, respectively, all the quantum numbers of the electronic and vibrational states of the whole system, and the excitation can either be localized on the molecule or on the surface. The function $\nabla_s U(\vec{r})$ is the change in potential energy at position $\vec{r}$ due to an infinitesimal movement of atom s. Since we are interested in the vibrational modes of the molecule, the unit movements $\vec{e}_{qs}$ of our interest are mainly localized at the molecule, while the single-electron state j can be either on the molecule or on the surface, and the same applies to state j'.

In principle, *ab initio* calculations, or other quantum chemical approach methods, could be used to evaluate these matrix elements, which would be able to capture the specific features of the molecule-surface interaction and allow for a detailed calculation of the Raman intensity in these hybrid molecule-2D material systems.

Although our aim here is not to calculate these matrix elements in detail, some considerations can be made about these matrix elements which will help understanding the overall properties of the Raman enhancement process. There are five straightforward possibilities for the relevant electron-phonon matrix elements: M_{HH}^{ep}, M_{LL}^{ep}, M_{SS}^{ep}, M_{HS}^{ep}, M_{LS}^{ep}, involving electron-phonon coupling between either the HOMO (H) or the LUMO (L) molecular orbitals and the surface (S). The first two matrix elements (M_{HH}^{ep}, M_{LL}^{ep}) are the usual electron-phonon coupling of the molecule, which give rise to the resonance Raman process for the isolated molecule. All Raman-active modes should have nonvanishing values for these matrix elements, in the sense of perturbation theory. The third possible term (M_{SS}^{ep}) represents a mixing between two different electronic states of the surface due to the vibration of atoms of the molecule when on the surface. We argue that if the interaction between the molecule and the surface is weak, the movement of atoms in the molecule should have a very weak effect on the electronic states of the surface, and thus the M_{SS}^{ep} term can be neglected. Finally, M_{HS}^{ep}, M_{LS}^{ep} represent a mixing between the electronic states of the molecule with those of the substrate due to the vibration of the atoms in the molecule.

Furthermore, we can assume that for a 2D surface, the matrix elements in Eqs. (6)–(8) are also independent of the electronic energy of the surface states. This approximation seems reasonable for an ideal 2D metal, for which the electronic density of states is approximately independent of the energy (within use of the effective mass approximation). These four optical matrix elements (M_{HH}^{ep}, M_{LL}^{ep}, M_{HS}^{ep}, M_{LS}^{ep}) can then be regarded approximately as constants which will determine the main contributions to the Raman-enhancement effect. From Eq. (11) it can be expected that for most systems the magnitude of M_{HS}^{ep} and M_{LS}^{ep} should be much smaller than that of M_{HH}^{ep} and M_{LL}^{ep}, especially for molecules weakly bound to the surface, for which the overlap between wave functions in the molecule and in the metal will be rather small. However, as we will show later, some Raman scattering

processes proportional to the M_{HS}^{ep} and M_{LS}^{ep} matrix elements can be doubly resonant and thus play an important role in the Raman-enhancement process.

2. Electron-radiation matrix elements

The matrix elements for the electron-photon interaction can be defined as

$$M_{\sigma jj'}^{er} = \sqrt{\frac{\hbar}{2V\epsilon_0\omega_\sigma}}\,\vec{e}_\sigma \cdot \int d^3r \, \psi_{j'}^*(\vec{r})\vec{\nabla}\psi_j(\vec{r}), \qquad (12)$$

with V the volume of the box containing the electromagnetic field, ϵ_0 the vacuum permittivity, and σ specifies the photon polarization. The long-wavelength approximation $\vec{Q}_{\text{photon}} = 0$ is considered. Again, the j and j' indices can, respectively, specify the electronic states localized in the molecule or in the surface. In this case there are also four relevant independent matrix elements M_{HS}^{er}, M_{LS}^{er}, M_{HL}^{er}, and M_{SS}^{ep}, which can also be considered as being independent of energy, to a first approximation. We can also, for the same reasons given above, expect from Eq. (12) that the matrix elements corresponding to electronic transitions within the surface (M_{SS}^{ep}) and within the molecule (M_{HL}^{ep}) will be much stronger than those involving transitions between the molecule and the surface. However, the magnitude of M_{HS}^{er} and of M_{LS}^{er} are extremely important for the Raman intensity since all relevant Raman processes involve either one or the other of these matrix elements and thus, in case both M_{HS}^{er} and M_{LS}^{er} vanish, the resonance Raman processes discussed in this work will make a negligible contribution to the Raman enhancement.

B. Resonance processes in 2D materials

We can now analyze the possible resonance processes involving a molecule and a 2D surface. For simplicity we will assume that in a weak interaction regime, there is a negligible charge transfer between the molecule and the surface, such that the HOMO state of the molecule will be fully occupied and the LUMO state is unoccupied. Note that we are only interested in terms for which there is a coupling between the molecule and the surface. Therefore, we should ignore all processes which occur exclusively at the surface and which therefore should have negligible effect on the molecular Raman scattering intensity.

Therefore, there are two possibilities for the initial electronic state i: the initial state can be either from the molecular HOMO state or from an occupied electronic state at the surface. For each of these terms, there are six possible processes for the electron and six processes for the hole, depending on the sequence of the possible states. In Fig. 2, we show the six possible electron mediated processes for each of the time-ordering situations. For example, the process named (rpr)-MMS represents a process for which an electron initially on the molecule (M) is scattered to another molecular state by absorbing electromagnetic radiation, this excited electron is then scattered to the surface (S) by creating a phonon, and is finally scattered back to the initial state by the emission of a photon.

It is interesting to comment that the (rrp)-SMS and (rpr)-SSM processes involve a transition between two
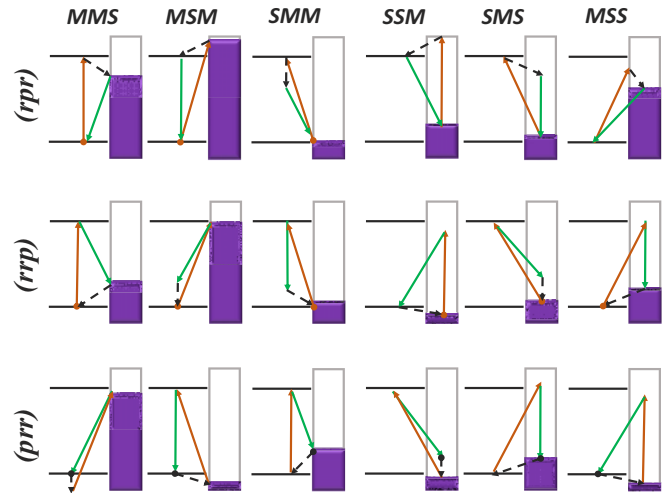

FIG. 2. (Color online) Possible resonance Raman processes for a molecule interacting with a 2D metallic substrate. Each process is labeled according to the time sequence of the electron-radiation and electron-phonon interaction, and according to the sequence of excited states possibly being on the molecule (M) or on the surface (S). Orange and green arrows represent the absorption and emission of a photon, respectively, while the black dashed line represents the creation of a phonon.

electronic states of the surface due to a vibration of the molecule, and thus depend on the M_{SS}^{ep} matrix element, which, as discussed in Sec. III A, can be regarded to be rather weak and can be neglected. However, we included such processes in the diagrams of Fig. 2 for completeness. Furthermore, although we have made no considerations about the occupation of the electronic molecular states when developing the diagrams in Fig. 2, it is clear that in most cases the involved electronic states of the molecule can be regarded as an occupied HOMO state and an unoccupied LUMO state. With this in mind, we can further limit the number of possible processes which can contribute significantly to the Raman scattering process. For example, processes such as the (rrp)-SMM involve a phonon mediated transition between an occupied state in the surface and also an occupied HOMO state in the molecule, which is forbidden by Pauli's exclusion principle.

Similar diagrams can be produced for the hole mediated processes (not shown here) and can also contribute to the Raman enhancement by 2D systems. Therefore, we see that the surface-molecule Raman process is in fact a sum of 36 different processes, each one having a different set of resonance conditions and a different dependence on the position of the Fermi energy. These processes can also interfere with each other leading to a rather complicated behavior.

Considering the great variety of different processes, each process with its own set of matrix elements and each with different dependencies on both laser excitation energy (E_{laser}) and Fermi energy (E_F), it becomes rather complicated to make a complete analysis of the Raman-enhancement process in 2D materials. Also, the fact that each of these terms can interfere constructively or destructively with the others adds even more complication to the analysis. However, although there are about 36 different processes that need to be taken into

account (the list of processes and their amplitudes is found in the Appendix), we can group together all terms which have the same set of matrix elements in the numerator. A more careful analysis of the different processes shows that there are 10 different combinations of the relevant matrix elements for the Raman-enhancement process, leading to 10 different terms which will be discussed below. Because the processes involved in each of these 10 terms share the same numerator, they cannot interfere with one another and the overall behavior of each of these 10 terms is independent of a formal knowledge about the matrix elements. The total magnitude of the Raman process can only be obtained when considering the sum of the 10 terms, with possible interference effects occurring between them.

The 10 possible processes listed below can be divided into three groups:

$$
\begin{aligned}
&\text{(I)}
\begin{cases}
LLS \rightarrow M_{SL}^{er} M_{LL}^{ep} M_{LS}^{er}; \\
HHS \rightarrow M_{SH}^{er} M_{HH}^{ep} M_{HS}^{er};
\end{cases} \\[2mm]
&\text{(II)}
\begin{cases}
LSH \rightarrow M_{HL}^{er} M_{LS}^{ep} M_{SH}^{er}; \\
\overline{LSH} \rightarrow M_{HS}^{er} M_{SL}^{ep} M_{LH}^{er}; \\
HSL \rightarrow M_{LH}^{er} M_{HS}^{ep} M_{SL}^{er}; \\
\overline{HSL} \rightarrow M_{LS}^{er} M_{SH}^{ep} M_{HL}^{er};
\end{cases} \quad (13) \\[2mm]
&\text{(III)}
\begin{cases}
LSS \rightarrow M_{SL}^{er} M_{LS}^{ep} M_{SS}^{er}; \\
\overline{LSS} \rightarrow M_{SS}^{er} M_{SL}^{ep} M_{LS}^{er} \\
HSS \rightarrow M_{SH}^{er} M_{HS}^{ep} M_{SS}^{er}; \\
\overline{HSS} \rightarrow M_{SS}^{er} M_{SH}^{ep} M_{HS}^{er},
\end{cases}
\end{aligned}
$$

where we used the fact that the matrices are Hermitian, $M_{BA} = M_{AB}^{*}$.

The division of the above 10 terms into the three categories [(I)–(III)] is made based on the dominant matrix element that is contributing to the intensity of each of the 10 terms. For example, category (I) is characterized by the magnitude of the leading contribution of the molecule-molecule electron-phonon matrix element, which is deemed to be much stronger than the molecule-surface electron-phonon matrix element in categories (II) and (III). Category (II) is characterized by its dependence on the electron-radiation scattering matrix element within the molecule, which in most cases should be larger than the electron-radiation matrix element coupling the molecule and the surface. On the other hand, terms in category (III) are characterized by their dependence on the electron-radiation scattering matrix element between states within the surface, which carries an extra dependence on the surface density of states. Again, this matrix element (M_{SS}^{er}) can, in many cases, be considered to be stronger than the electron-radiation matrix elements coupling the molecule and the surface (M_{LS}^{er}, M_{HS}^{er}).

C. Enhancement factors

One of the most controversial subjects in both experimental and theoretical approaches for the study of the SERS effect is on the definition of the enhancement factors. The situation is not different for the model for the Raman-enhancement effects discussed here. A simple definition of the enhancement factor

would be the ratio between the calculated Raman intensity for an adsorbed molecule and the calculated intensity for an isolated molecule. The problem lies in the fact that the model described by Eqs. (6)–(8) can only be applied for the isolated molecule if the photon energy is nearly resonant with the HOMO-LUMO transition energy. In that case, the Raman scattering amplitude is given by the well-known expression

$$
W_{MMM} = \frac{M_{HL}^{er}\left(M_{LL}^{ep} - M_{HH}^{ep}\right)M_{LH}^{er}}{(E_L - E_H + \hbar\omega_q - \hbar\omega_0)(E_L - E_H - \hbar\omega_0)},
$$
(14)

where the MMM subscript indicates that W_{MMM} corresponds to a process involving only the electronic states of the molecule (and is thus independent of the interaction with the surface). However, for laser energies far from the HOMO-LUMO transition energy, Eq. (14) is no longer valid, and all off-resonance terms which have been neglected start playing an important role. Furthermore, evaluating these enhancement factors depends also on how the interaction with the surface affects both the electronic states and energies of the molecule, thereby affecting its resonance condition while on the surface.

In this work, we focus only on the surface mediated processes, thereby neglecting the resonance process of the molecule itself, which in an experimental setup will make an important contribution to the Raman intensity. In this sense, in the following section we do not calculate enhancement factors, but we only consider the physics behind the contribution of the interaction between the molecule and the surface to the Raman scattering process. This will give important insights into the underlying process responsible for the Raman enhancement and will guide us on how we can maximize this surface-enhancement effect.

IV. RESULTS

In this section we show the application of the theory of Raman resonance developed above to two simple 2D materials. First, we analyze the Raman-enhancement properties of an ideal 2D metal in order to elucidate the general principles governing this effect. Following this, we apply the theory to graphene, where the Raman-enhancement effect has been observed experimentally and for which the theoretical framework presented here may be applied.

A. Raman enhancement in an ideal 2D metal

Before studying the GERS effect in detail, we will start our discussion on a simpler system, which we can refer to as an ideal 2D metal. An ideal 2D metal is one which can be regarded as a 2D electron gas for which the Fermi level is well above the zero energy and with an arbitrarily high work function. Due to the 2D nature of the metal, the density of states is a constant throughout the whole energy range of interest.

In Fig. 3 we show the calculated Raman intensities as a function of both the laser excitation energy E_{laser} and the Fermi energy E_F considering a two-state molecule interacting with an ideal 2D metal. The density of states is considered to be constant throughout the whole energy range (from -5 to 5 eV) and all the matrix elements are considered to be equal to 1, with the exception of $M_{SS}^{ep} = 0$ which, as discussed above,
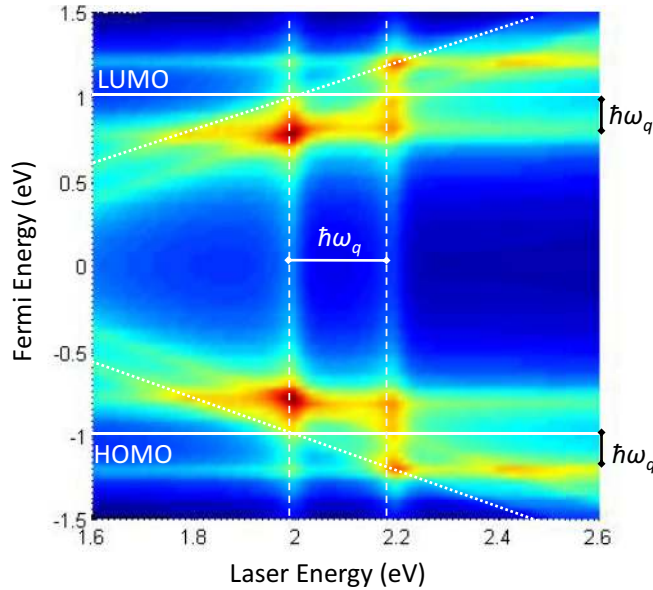
FIG. 3. (Color online) The total Raman intensity as a function of the excitation photon energy $E_{laser} = \hbar\omega_0$ and of the Fermi energy E_F considering all the relevant matrix elements to be unity. All energies are in units of electron volts. The phonon energy is $\hbar\omega_p = 0.2$ eV and a homogeneous Raman linewidth broadening of $\gamma = 0.03$ eV was considered. The solid horizontal lines are guides to the eye, showing the position of the HOMO and LUMO states, while the dashed vertical lines correspond to the energies of the resonances with the incident (left) and scattered (right) photons. The diagonal dotted lines correspond to the condition for which the laser energy matches the energy difference between the E_F and the energy of the HOMO or LUMO states.

is neglected throughout this work. Figure 3 shows the result for the sum between all the terms in categories (I)–(III) in Eq. (13), and since all the matrix elements are considered to be equal, the results in Fig. 3 disregard some possible important interferences between the different processes. However, in spite of that, Fig. 3 can be used to obtain some insight into what role is played by the laser excitation energy $E_{laser} = \hbar\omega_0$ and by the Fermi energy E_F in the intensity enhancement process. For example, it can be readily seen that larger enhancements occur for the following four conditions:

$$
\begin{aligned}
&\text{(i) } \hbar\omega_0 = E_L - E_H \quad \text{or} \quad \hbar\omega_0 = E_L - E_H + \hbar\omega_q, \\
&\text{(ii) } E_F = E_H \pm \hbar\omega_q \quad \text{or} \quad E_F = E_L \pm \hbar\omega_q, \\
&\text{(iii) } \hbar\omega_0 = E_F - E_H \quad \text{or} \quad \hbar\omega_0 = E_F - E_H + \hbar\omega_q, \\
&\text{(iv) } \hbar\omega_0 = E_L - E_F \quad \text{or} \quad \hbar\omega_0 = E_L - E_F - \hbar\omega_q,
\end{aligned}
\tag{15}
$$

where E_H and E_L are the energies of the HOMO and LUMO states of the molecule, respectively, E_F is the Fermi energy of the metal, and $\hbar\omega_0 = E_{laser}$ is the laser excitation energy.

Condition (i) in Eq. (15) is well known and is related to the resonance between the molecular electronic transition with either the incident light or the scattered light, respectively. The interesting and rather impressive result is that in the case of the molecule interacting with an ideal 2D metal, the condition of optimal resonance for the Fermi energy [condition (ii)] occurs when the Fermi energy is above or below one of the
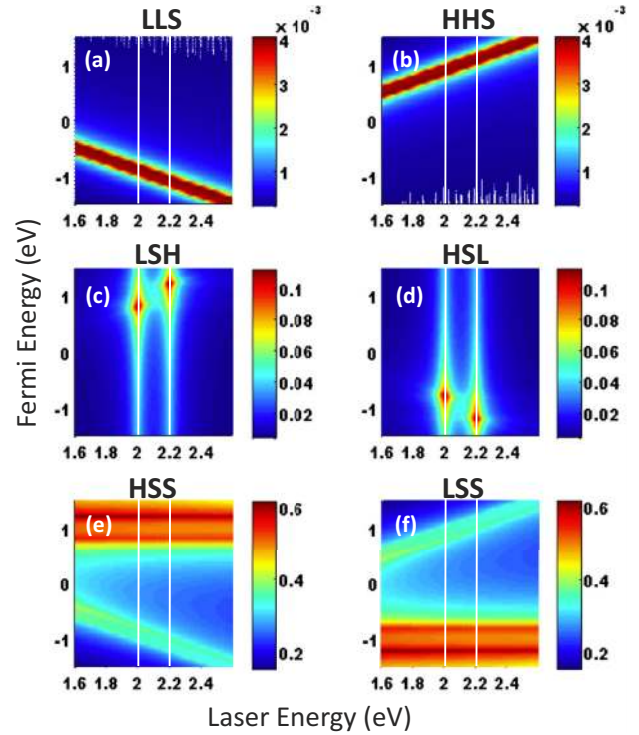

FIG. 4. (Color online) Absolute Raman scattering amplitude as a function of the excitation photon energy $E_{laser} = \hbar\omega_0$ and of the Fermi energy E_F for the (a) LLS, (b) HHS, (c) LSH, (d) HSL, (e) HSS, and (f) LSS processes. The horizontal lines on each panel represent $E_L - E_H = 2$ eV (leftmost line) and $E_L - E_H + \hbar\omega_q$ (rightmost line) where E_L and E_H are the LUMO and HOMO energies and $\hbar\omega_p = 0.2$ eV is the phonon energy. A homogeneous broadening of $\gamma = 0.03$ eV was considered. The electron density of states of the 2D metal was considered to be unity $g(E) = 1$.

molecular electronic levels by exactly the phonon energy, and *not when the Fermi energy coincides with the electronic levels themselves*. This result can be regarded as one of the most important results of this paper, which suggests that gating effects on the enhancement factors in Raman enhancement studies in 2D materials should be strongly dependent on the frequency of the observed Raman peak. As we will show in the following, the same consideration is valid for the graphene-enhancement process (GERS). Finally, there are the conditions (iii) and (iv) for enhancement, which happen when E_{laser} matches the energy difference between the Fermi energy of the metal and the HOMO or LUMO states of the molecule plus or minus the phonon energy $\hbar\omega_q$.

Suppressing important interference effects is not the only consequence of disregarding the differences in the electron-phonon and electron-photon matrix elements for the processes contributing to the Raman-enhancement effect by a 2D metal. Also, the relative magnitudes of the processes will be different from one another, depending on the magnitude of the matrix elements, which can make the total dependence of the enhancement to favor different behaviors. To better understand this, we show in Fig. 4 the absolute Raman scattering amplitude for the processes in categories (I)–(III) of Eq. (13) for comparison. We first would like to note that the maximum amplitude of the category (I) terms is about 25 times weaker than that of
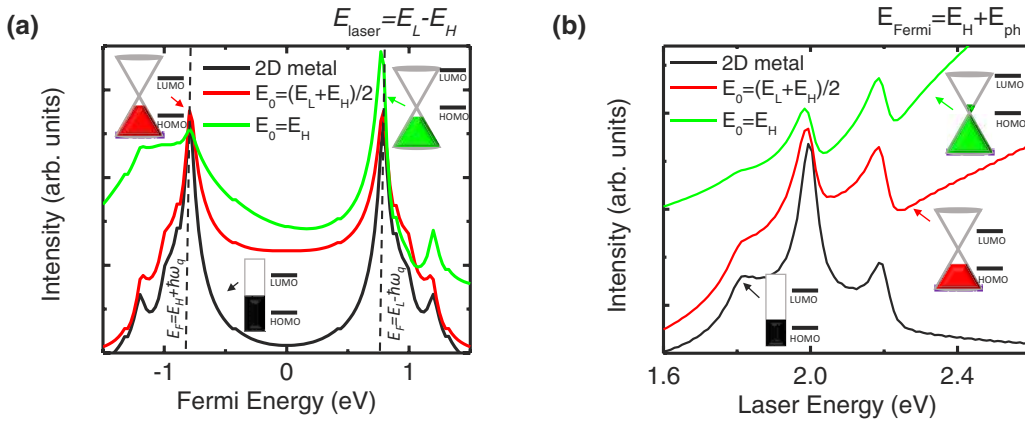
FIG. 5. (Color online) (a) Raman intensity as a function of the Fermi energy for $E_{laser} = E_L - E_H$ considering an ideal 2D metal (black), graphene with $E_0 = (E_L - E_H)/2$ (red), and graphene with $E_0 = E_H$ (green) as the enhancing surface. (b) Raman intensity as a function of laser excitation energy for $E_F = E_H + \hbar\omega_q$. We here consider $E_H = -1$ eV, $E_L = 1V$ eV, $\hbar\omega_q = 0.2$ eV, and a homogeneous broadening of $\gamma = 0.03$ eV.

the category (II) terms and this conclusion is independent of the surface density of states. The reason for the strong relative intensities of the terms in category (II) compared to those in category (I) is that in category (II) there is the possibility of a double resonance, for which both terms in the denominator vanish. Category (III) terms also include the possibility of such a double resonance occurrence and should therefore result in a relevant contribution to the Raman enhancement. It is interesting to note that the intensity of the category (III) contribution is proportional to the fourth power of the electron density of states in the 2D surface, while terms in categories (I) and (II) depend on the square of the density of states (see the Appendix). This means that for 2D metals with a larger density of states, the category (III) terms should play an important role.

Let us now analyze each case separately. In Figs. 4(a) and 4(b) we show the absolute Raman scattering amplitudes for the LLS and HHS terms in category (I) of Eq. (13) as a function of E_F and E_{laser} using the same conditions as are used in Fig. 3. It can be seen that the main contribution arises when conditions (iii) and (iv) of Eq. (15) are met. For the LSH and HSL terms in category (II) [Figs. 4(c) and 4(d), respectively], the enhancement occurs mainly when the laser energy is resonant with the molecular electronic transition $E_{laser} = E_L - E_H$, but there is an extra enhancement when $E_F = E_H + \hbar\omega_q$ for the LSH term and when $E_F = E_L - \hbar\omega_q$ for the HSL term. For the category (III), regarding terms HSS and LSS [Figs. 4(e) and 4(f), respectively], there are relevant contributions coming from conditions (ii), (iii), and (iv) of Eq. (15).

It is also necessary to comment on the underlying physics responsible for the Fermi-energy dependence of the Raman intensity enhancement. First we would like to point out that this dependence does not follow a Lorentzian line shape, as expected in a resonant Raman experiment. To illustrate this, we show, as a black curve in Fig. 5(a), the Raman intensity as a function of the Fermi energy for the condition $E_{laser} = E_L - E_H$, considering the enhancing surface to be an ideal 2D metal. The HOMO and LUMO energies are assumed to be at -1 and 1 eV, such that E_{laser} is in the visible range (2 eV). For the 2D metal case, it can be seen that there are two strong peaks, one at $E_F = E_H + \hbar\omega_q = -0.8$ eV and the other one at

$E_F = E_L - \hbar\omega_q = 0.8$ eV. Two other smaller peaks appear in Fig. 5(a) at $E_F = E_H - \hbar\omega_q = -1.2$ eV and $E_F = E_L + \hbar\omega_q = 1.2$ eV corresponding to the resonance condition (ii) of Eq. (15).

To understand this enhancement effect shown in Fig. 5(a), it is necessary to recall that the total Raman process is obtained by summing the amplitudes of all possible scattering processes. If the Fermi energy is far away from the HOMO and LUMO states, there is a manifold of electronic states near the HOMO and LUMO states which can contribute to the Raman scattering process. A few of these states may happen to be in perfect resonance with one of the possible Raman processes, as described in the Appendix. However, for each possible Raman process there are also some states with a slightly larger energy than that of the perfect resonance condition and some with a slightly smaller energy. The contributions from the states above the resonant condition and below the resonant condition tend to cancel each other, and since the density of states and the matrix elements for these processes for the special case of the ideal 2D metal are all considered to be independent of the energy, this cancellation is perfect for this particular case. Therefore, in this idealized situation, *if the Fermi energy is far from both HOMO and LUMO states, the density of states and matrix elements are constant, there should be absolutely no CT-SERS enhancement in 2D metals*. However, when the Fermi energy approaches the condition of resonance for one of the Raman processes, Pauli exclusion prevents the states which are below the resonance condition from canceling out the contribution from the states above the resonance condition, thus increasing the expected total Raman intensity. This quantum interference effect is similar to that observed for the G-band Raman peak in graphene, as predicted by Basko and later observed experimentally [25–27].

Lombardi *et al.* have shown that, within Albrecht's approach for the charge-transfer SERS effect, the Raman scattering amplitude for an ideal 2D metal with constant matrix elements shows a logarithmic dependence on the Fermi energy [21]. Within the time-dependent approach presented here, the situation is more complicated due to the fact that the different terms contributing to the Raman scattering process have a different dependence on the Fermi energy. For example,

considering the ideal 2D metal band with a density of states given by

$$g(E) = \begin{cases} g, & E_A < E < E_B, \\ 0, & E > E_A \text{ and } E < E_B \end{cases} \tag{16}$$

the (rpr)-$MMSe$ term (see Table I in the Appendix), belonging to category I, becomes

$$W_{MMSe}^{(rpr)}(\text{2D}) = g \frac{M_{HL}^{er} M_{LS}^{ep} M_{SH}^{er}}{E_L - E_H - \hbar\omega_0} \ln \frac{E_B - E_H + \hbar\omega_q - \hbar\omega_0}{E_F - E_H + \hbar\omega_q - \hbar\omega_0}, \tag{17}$$

which has a simple logarithm dependence peaked at $E_F = E_H + \hbar\omega_0 - \hbar\omega_q$ similar to that predicted by Lombardi *et al.* [21]. However, for the category II (rpr)-$SMMe$ term, for example, the logarithmic dependence is slightly different,

$$W_{SMMe}^{(rpr)}(\text{2D}) = g \frac{M_{SL}^{er} M_{LL}^{ep} M_{LS}^{er}}{\hbar\omega_q} \ln \frac{E_L - E_F + \hbar\omega_q - \hbar\omega_0}{E_L - E_F \hbar\omega_0}, \tag{18}$$

having two peaks at $E_F = E_L + \hbar\omega_q - \hbar\omega_0$ and $E_F = E_L - \hbar\omega_0$. To obtain the above expression, we have made the following approximation: $|E_L - E_A| \gg \hbar\omega_0 + \omega_q$.

For some terms, the difference is even more striking. For example, for the category III (prr)-$MSSe$ term the Raman scattering amplitude has a dilogarithmic behavior, given by

$$\begin{aligned} W_{MSSe}^{(prr)}(\text{2D}) &= g^2 M_{SS}^{er} M_{SL}^{er} M_{LS}^{ep} \\ &\times \left[\text{Li}_2 \frac{E_B + E_L - \hbar\omega_0}{E_L - E_A + \hbar\omega_q} + \text{Li}_2 \frac{E_F + E_L - \hbar\omega_0}{E_L - E_F + \hbar\omega_q} \right. \\ &\left. - \text{Li}_2 \frac{E_F + E_L - \hbar\omega_0}{E_L - E_A + \hbar\omega_q} - \text{Li}_2 \frac{E_B + E_L - \hbar\omega_0}{E_L - E_F + \hbar\omega_q} \right], \end{aligned} \tag{19}$$

where Li_2 stands for the polylogarithm or Jonquière's function of order 2, also known as dilogarithmic function.

It should be mentioned here that in order to obtain the expressions above, constant matrix elements were considered. Since this is usually not the case, the logarithmic behavior predicted here can only be regarded qualitatively. For a quantitative analysis, it is necessary to perform a detailed calculation of the Raman intensity in which all the relevant terms in Table I are taken into consideration. Nevertheless, the analytical expressions can be of considerable help in understanding some of the properties of the Raman scattering process in such systems.

If we define $\overline{M}_{MM}^{ep}$ and $\overline{M}_{MM}^{er}$ as a measure of the overall strength of the molecular electron-phonon and electron-radiation matrix elements, $\overline{M}_{MS}^{ep}$ and $\overline{M}_{MS}^{er}$ as the strength of the molecule-surface electron-phonon and electron-radiation matrix elements and $\overline{M}_{SS}^{er}$ as the strength of the electron-radiation matrix element between states in the surface, we can use the above expressions to evaluate for each specific situation, which of the categories will be more relevant. To accomplish this, we note that at the perfect double resonance condition the intensities of each of the terms will be determined by the following factors: $\alpha_{(\text{I})} = \overline{M}_{MM}^{ep} \overline{M}_{MS}^{er} \overline{M}_{MS}^{er}/\hbar\omega_q$,

$\alpha_{(\text{II})} = \overline{M}_{MS}^{ep} \overline{M}_{MM}^{er} \overline{M}_{MS}^{er}/\gamma$, and $\alpha_{(\text{III})} = \overline{g} \overline{M}_{MS}^{ep} \overline{M}_{SS}^{er} \overline{M}_{MS}^{er}$, in which the constant γ is the broadening of the electronic states and is related to the lifetime of the excitations, while $\overline{g}$ is the constant density of states of the 2D metal. Although this analysis is performed here only for specific terms in each of the categories, similar qualitative results are obtained for the other terms.

Having a previous knowledge of the dominant matrix elements, lifetimes and the density of states can lead to important insights into which processes could be more relevant for particular situations and thus to determine the conditions for which the enhancement is maximized. For example, for systems in which the electron-photon matrix elements for transitions between different surface states are weak, $M_{SS}^{er} \to 0$, then the terms in category (III) can be safely disregarded.

B. Graphene-enhanced Raman spectroscopy process

The first and most prominent 2D material that has been shown experimentally to produce an enhancement effect in the molecular Raman spectra was graphene [1]. In the case of graphene, this effect has been named graphene-enhanced Raman spectroscopy, or GERS [2]. The explanation for the Raman intensity enhancement when a molecule interacts with graphene is similar to that developed in the previous section, with the important difference that the electronic density of states in graphene is not constant, but instead it increases approximately as $g(E) = \beta|E - E_0|$, where E_0 is the charge neutrality energy and $\beta = 2/(\pi\hbar^2 v_f^2)$, with v_f being the Fermi velocity of carriers in graphene (on the order of 10^6 m/s) [28]. This behavior adds an extra parameter for describing the Raman-enhancement effect, which is the relative position of the E_0 with respect to the energy levels of the molecule. This finding indicates that the GERS effect is strongly dependent on the exact electronic structure of the molecule and not only on the energy difference between the HOMO and LUMO states. Therefore, molecules which have similar resonance energies may show strikingly different enhancement factors and different physical behaviors, generally.

In Fig. 5(a) we compare the Fermi-energy dependence of the Raman intensity for the case of graphene as the enhancing surface (shown in red and in green) with that of the ideal 2D metal (in black). For the red curve we have considered that the charge neutrality energy in graphene (also known as the Dirac point) is precisely in the middle of the HOMO-LUMO gap, while the green curve is for the case when the charge neutrality point (E_0) coincides with the HOMO state. In the first case, $E_0 = (E_H - E_L)/2$, the electron-hole symmetry is preserved such that the Raman intensity for processes involving the HOMO and LUMO states is symmetric, just as in the case of the 2D metal. There are, however, a few differences between the enhancement in graphene and in the 2D metal. The first difference is that for the GERS effect, the Raman intensity for $E_H < E_F < E_L$ is not completely canceled out, but remains about half of the peak values (obtained for $E_F = E_H + \hbar\omega_q$ and $E_F = E_L - \hbar\omega_q$). This is explained by the fact that the density of states in graphene is not constant, but rather increases linearly with the energy so that the contributions from above and below the resonance condition for each Raman process cannot cancel out completely. This might be one of the

reasons why graphene is an especially good surface material for the observation of Raman-enhancement phenomena. A similar effect is obtained in graphene even if the neutrality point is not exactly at the middle of the HOMO-LUMO gap, as shown in green in Fig. 5(a), with the difference that in the case for which the E_0 is closer to E_H, the electron-hole symmetry is broken and the Raman intensity for $E_F \sim E_H$ is weaker since the carrier density of states goes to zero at the charge neutrality point. A corresponding behavior is observed for $E_0 = E_L$ (not shown here).

Finally, we examine the laser excitation energy dependence of the Raman intensity for the case where $E_F = E_H + \hbar\omega_q$ in Fig. 5(b). For the ideal 2D metal, with a constant density of states, there is a strong peak when the photon energy matches the molecular electronic transition $E_{\text{laser}} = E_L - E_H = 2$ eV and two weaker peaks appear at $E_{\text{laser}} = E_L - E_H \pm \hbar\omega_q$. The presence of the peak below the molecular transition energy is not expected for an isolated molecule and arises from *hole* mediated processes, such as those depicted in Figs. 1(d)–1(f). These processes can only be described in terms of the complete time-dependent perturbation theory presented here and thus are not predicted within Lombardi's theory for the CT-SERS effect. For photon energies much larger than the molecular electronic transition, the Raman intensity falls rapidly due to the fact that contributions from the 2D metal states above that energy cancel each other, as discussed above. The same is not true for the case of graphene, for which the Raman intensity increases with increasing laser excitation energy both for the case where E_0 is in the middle of the gap and when E_0 coincides with the HOMO state.

V. APPLICATIONS

The actual Raman enhancement observed for the molecule will be affected by a combination of factors, such as the luminescence quenching observed by Xie *et al.* [7] and the different enhancement processes, including the electric field enhancement due to multiple scattering processes proposed by Jung *et al.* [3], and the double resonance Raman scattering process discussed here. A combination between the different favorable processes leads to stronger enhancements which allows for a corresponding improved resolution for the observed Raman spectra of molecules. Also, since the process discussed here involves the electronic states of both the molecule and the surface, the Raman spectroscopy of molecules adsorbed onto 2D material can also give important information about the electronic properties of the molecule, of the surface, and about their interactions. This technique might also prove to provide a useful tool for investigating the nature of the molecule-surface interaction.

To better profit from the Raman enhancement by 2D materials and to extract valuable information about the molecule-surface interaction, it is essential that the Raman intensity of the system can be calculated in further detail than what is given in this general overview of the enhancement process. For such a more detailed discussion, it is necessary that both the electronic properties of the molecule and of the surface, as well as the matrix elements discussed in Sec. III A, are known. Some of the well-known properties of the CT-SERS, such as the first-layer interaction [2,20] and the

selection rules for the enhancement of particular vibrations, are related to these properties.

Ideally, an accurate description of the Raman scattering enhancement for the molecules adsorbed on 2D materials can be accomplished if the electronic and vibrational properties of the molecule-2D material hybrid system are well known. For this, first-principles calculations could be performed for the molecule interacting with the 2D material. In this case, the expressions such as those given in Eqs. (11) and (12) can be used to estimate the matrix elements. Finally, the Raman scattering intensities for the molecule-2D material system can then be calculated for any given laser excitation energy and Fermi energy by using the complete set of equations summarized in the Appendix, or by selecting the more relevant subsets of equations, depending on the nature of the molecule-surface interaction. The calculated results can then be compared to the experiments, leading to a better understanding of the interaction between molecules and the 2D materials.

In some cases, computational limitations prevent the accurate calculation of the electronic energies or matrix elements for the hybrid system composed of the molecules interacting with the 2D material. In this situation, if the matrix elements and energies of the independent molecule and 2D material are known individually, the interaction between the molecule and the surface can still be investigated by regarding the matrix elements for the surface-molecule interaction as fitting parameters and then the resulting parameters can be used to make further progress in explaining the experimental results. In this way, new insights are gained for advancing our understanding of the interaction between the molecule and the 2D material.

Furthermore, although we have focused in this work mainly on two simple cases of 2D materials (an ideal 2D metal and graphene), the formalism developed here is quite general and can be extended to other types of 2D materials, such as hexagonal boron nitride (h-BN), MoS_2, and other transition-metal dichalcogenides. However, the Raman process in such systems can be governed by excitonic effects, which can greatly modify the observed behaviors.

VI. CONCLUSIONS

In this work, we have developed a time-dependent perturbation theory approach for explaining the Raman enhancement effect observed in 2D materials. The approach used here is based on considering the enhancement as coming from a resonance Raman process involving the electronic states of both the molecule and the surface. Expressions for all the relevant time-ordered Raman scattering processes contributing to the Raman scattering intensity are considered and their role in the Raman scattering of adsorbed molecules is discussed. We have shown that the interaction between the molecule with the 2D material may result in enhanced Raman scattering intensities. The conditions for maximizing the Raman enhancement are discussed. For example, we show that for ideal 2D metals, with a constant density of electronic states, the Raman intensity is a maximum when the Fermi energy of the metal matches the HOMO or LUMO molecular orbital energies of the molecule plus or minus the phonon energy. The enhancement is shown to decrease quickly as the Fermi level moves away

from the HOMO and LUMO state energies. In the case of graphene, for which the density of states increases linearly with energy, as measured from the charge neutrality point, the Raman intensity does not completely vanish for values of E_F between the HOMO and LUMO molecular orbital energies; either the Raman intensity evolves towards a constant nonzero value for $E_H < E_F < E_L$, but decreases quickly for $E_F \gg E_{\text{LUMO}}$ and $E_F \ll E_{\text{HOMO}}$. A large scattering intensity is also shown to occur when the laser excitation energy matches the energy difference between the Fermi energy of the surface and the energy of the HOMO or LUMO states of the molecule. The model proposed here may shed light on increasing a qualitative understanding of the laser energy and Fermi energy dependence of the observed graphene-enhanced Raman spectroscopy effects [1,2,6]. Finally, we should point out that with this work we have developed an appropriate framework for calculating the Raman-enhancement effects of different molecules interacting with 2D materials, which will lead to more accurate predictions and a deeper understanding of these interesting effects.

ACKNOWLEDGMENTS

APPENDIX

Here, we explain how we can obtain the contribution from all of the possible Raman scattering processes. For clarity, we have labeled each process according to the different time ordering of electron radiation (r) and electron phonon interaction (p), to the location of the electronic states involved

in the scattering process (M for molecule states and S for surface states) and also for whether the process is for electron (e) or hole (h) excitation. For example, for obtaining the scattering amplitude for the (rpr)-$MMSe$ process we take the term in Eq. (6) related to the electron process (e), which is the one weighted by the factor $\chi_{kk'}^{iq}$ [Eq. (9)]. We then consider that the initial state i is a molecular (M) state, the first intermediate state k is also a molecular state (M) and the second intermediate state is a surface state (S). For the (rpr)-$MMSh$ process, we make the same consideration but choose the term in Eq. (6) which is weighted by the factor $\xi_{kk'}^{iq}$ [Eq. (10)], which corresponds to hole (h) mediated processes.

For the (rpr)-$MMSe$ process, the Raman amplitude is weighted by the factor $\chi_{kk'}^{iq}$ [Eq. (9)] so that the initial state has to be the HOMO state, which is occupied ($i = \text{HOMO}$), the first intermediate state must be the LUMO state which is assumed to be unoccupied ($k = \text{LUMO}$). For the MMS process, the second intermediate state k' can be any of the unoccupied states of the surface, and the total amplitude of this (rpr)-MMS term is given by summing the contributions from all k' states. The summation over states k' can be transformed into an integral over the possible electronic energies by defining the density of electronic states $g(E) = \sum_{k'} \int dE \, \delta(E - E_{k'})$, where k' covers all possible electronic states of the surface. The amplitude for the (rpr)-$MMSe$ contribution to the Raman amplitude takes the form

$$W_{(rpr)\text{-}MMSe}$$

$$= \int dE [1 - f(E - E_F)] g(E)$$

$$\times \frac{M_{HS}^{er}(E) M_{SL}^{ep}(E) M_{LH}^{er}}{(E_L - E_H - \hbar\omega_0)(E - E_H + \hbar\omega_q - \hbar\omega_0)}, \quad \text{(A1)}$$

TABLE I. Expressions for all relevant surface-enhanced Raman processes considering a two-state molecule interacting with a general 2D surface. The values E_L, E_H, $\hbar\omega_0$, and $\hbar\omega_q$ are, respectively, the energies for the LUMO and HOMO states of the molecule, the incident laser and the phonon involved with the Raman process. For compactness, we have defined $\mathcal{G}(E) = f(E - E_F) g(E)$ and $\bar{\mathcal{G}}(E) = [1 - f(E - E_F)] g(E)$ where $g(E)$ is the electronic density of states of the surface and $f(E - E_F)$ is the Fermi-Dirac distribution function for a given Fermi energy (E_F).

	(rpr)	(rrp)	(prr)
$MMSe$	$\int dE\, \bar{\mathcal{G}}(E) \frac{M_{HS}^{er}(E) M_{SL}^{ep}(E) M_{LH}^{er}}{(E_L - E_H - \hbar\omega_0)(E - E_H + \hbar\omega_q - \hbar\omega_0)}$	$\int dE\, \bar{\mathcal{G}}(E) \frac{M_{HS}^{ep}(E) M_{SL}^{er}(E) M_{LH}^{er}}{(E_L - E_H - \hbar\omega_0)(E - E_H - \hbar\omega_q)}$	$\int dE\, \bar{\mathcal{G}}(E) \frac{M_{HS}^{er}(E) M_{SH}^{er}(E) M_{HH}^{ep}}{(E - E_H + \hbar\omega_q - \hbar\omega_0)(\hbar\omega_q)}$
$MMSh$	(Off resonance)	(Pauli blocking)	(Pauli blocking)
$MSMe$	$\int dE\, \bar{\mathcal{G}}(E) \frac{M_{HL}^{er} M_{LS}^{ep}(E) M_{SH}^{er}(E)}{(E - E_H - \hbar\omega_0)(E_L - E_H - \hbar\omega_0)}$	$\int dE\, \bar{\mathcal{G}}(E) \frac{M_{HH}^{ep} M_{HS}^{er}(E) M_{SH}^{er}(E)}{(E - E_H - \hbar\omega_0)(-\hbar\omega_q)}$	$\int dE\, \bar{\mathcal{G}}(E) \frac{M_{HL}^{er} M_{LS}^{er}(E) M_{SH}^{ep}(E)}{(E_L - E_H + \hbar\omega_q - \hbar\omega_0)(E - E_H + \hbar\omega_q)}$
$MSMh$	$\int dE\, \mathcal{G}(E) \frac{M_{SL}^{er}(E) M_{HS}^{ep}(E) M_{LH}^{er}}{(E_L - E + \hbar\omega_q - \hbar\omega_0)(E_L - E_H - \hbar\omega_0)}$	$\int dE\, \mathcal{G}(E) \frac{M_{SL}^{ep}(E) M_{HS}^{er}(E) M_{LH}^{er}}{(E_L - E_H - \hbar\omega_0)(E_L - E - \hbar\omega_q)}$	(Off resonance)
$SMMe$	$\int dE\, \mathcal{G}(E) \frac{M_{SL}^{er}(E) M_{LL}^{ep} M_{LS}^{er}(E)}{(E_L - E - \hbar\omega_0)(E_L - E + \hbar\omega_q - \hbar\omega_0)}$	(Pauli blocking)	(Pauli blocking)
$SMMh$	$\int dE\, \mathcal{G}(E) \frac{M_{HL} M_{SH}^{ep}(E) M_{LS}^{er}(E)}{(E_L - E_H + \hbar\omega_q - \hbar\omega_0)(E_L - E - \hbar\omega_0)}$	(Off resonance)	$\int dE\, \mathcal{G}(E) \frac{M_{HL}^{er} M_{SH}^{er}(E) M_{LS}^{ep}(E)}{(E_L - E_H + \hbar\omega_q - \hbar\omega_0)(E_L - E + \hbar\omega_q)}$
$SSMe$	$\int dE\, dE'\, \bar{\mathcal{G}}(E') \mathcal{G}(E) \frac{M_{SL}^{er}(E) M_{LS}^{ep}(E') M_{SS}^{er}(E', E)}{(E' - E - \hbar\omega_0)(E_L - E + \hbar\omega_q - \hbar\omega_0)}$	$\int dE\, dE'\, \bar{\mathcal{G}}(E') \mathcal{G}(E) \frac{M_{SL}^{ep}(E) M_{LS}^{er}(E') M_{SS}^{er}(E', E)}{(E' - E - \hbar\omega_0)(E_L - E - \hbar\omega_q)}$	(proportional to M_{SS}^{ep})
$SSMh$	(proportional to M_{SS}^{ep})	$\int dE\, dE'\, \mathcal{G}(E') \mathcal{G}(E) \frac{M_{SL}^{er}(E') M_{SS}^{er}(E', E) M_{LS}^{er}(E)}{(E_L - E - \hbar\omega_0)(E_L - E' - \hbar\omega_q)}$	$\int dE\, dE'\, \mathcal{G}(E') \mathcal{G}(E) \frac{M_{SL}^{er}(E') M_{SS}^{er}(E', E) M_{LS}^{ep}(E)}{(E_L - E' + \hbar\omega_q - \hbar\omega_0)(E_L - E + \hbar\omega_q)}$
$SMSe$	$\int dE\, dE'\, \bar{\mathcal{G}}(E') \mathcal{G}(E) \frac{M_{SS}^{er}(E, E') M_{SL}^{ep}(E') M_{LS}^{er}(E)}{(E_L - E - \hbar\omega_0)(E' - E + \hbar\omega_q - \hbar\omega_0)}$	(proportional to M_{SS}^{ep})	$\int dE\, dE'\, \bar{\mathcal{G}}(E') \mathcal{G}(E) \frac{M_{SS}^{er}(E, E') M_{SL}^{er}(E') M_{LS}^{ep}(E)}{(E' - E + \hbar\omega_q - \hbar\omega_0)(E_L - E + \hbar\omega_q)}$
$SMSh$	$\int dE\, dE'\, \bar{\mathcal{G}}(E') \mathcal{G}(E) \frac{M_{HS}^{er}(E') M_{SH}^{ep}(E) M_{SS}^{er}(E', E)}{(E' - E - \hbar\omega_0)(E' - E_H + \hbar\omega_q - \hbar\omega_0)}$	$\int dE\, dE'\, \bar{\mathcal{G}}(E') \mathcal{G}(E) \frac{M_{HS}^{er}(E') M_{SH}^{er}(E) M_{SS}^{ep}(E', E)}{(E' - E - \hbar\omega_0)(E' - E_H - \hbar\omega_q)}$	(Off resonance)
$MSSe$	(proportional to M_{SS}^{ep})	$\int dE\, dE'\, \mathcal{G}(E') \bar{\mathcal{G}}(E) \frac{M_{HS(E')}^{ep} M_{SS}^{er}(E', E) M_{SH}^{er}(E)}{(E - E_H - \hbar\omega_0)(E' - E_H - \hbar\omega_q)}$	$\int dE\, dE'\, \bar{\mathcal{G}}(E') \bar{\mathcal{G}}(E) \frac{M_{HS}^{er}(E') M_{SS}^{er}(E', E) M_{SH}^{ep}(E)}{(E' - E_H + \hbar\omega_q - \hbar\omega_0)(E' - E_H + \hbar\omega_q)}$
$MSSh$	$\int dE\, dE'\, \bar{\mathcal{G}}(E') \mathcal{G}(E) \frac{M_{SS}^{er}(E', E) M_{HS}^{ep}(E) M_{SH}^{er}(E')}{(E' - E_H - \hbar\omega_0)(E' - E + \hbar\omega_q - \hbar\omega_0)}$	~ 0 proportional to M_{SS}^{ep}	$\int dE\, dE'\, \bar{\mathcal{G}}(E') \mathcal{G}(E) \frac{M_{SS}^{er}(E, E') M_{HS}^{er}(E) M_{SH}^{ep}(E')}{(E' - E + \hbar\omega_q - \hbar\omega_0)(E' - E_H + \hbar\omega_q)}$

where E_L, E_H, and E are the LUMO, HOMO, and surface state energies, respectively. In reality, these energies should have both a real and an imaginary part, where the latter causes a broadening to the resonance, and yields the lifetime of these states. In this expression, and in the subsequent ones listed below, we have omitted the imaginary parts of the excitation energies.

For the (rpr)-$MMSh$ process, involving the hole excitation, the Raman intensity is weighted by the function $\xi_{kk'}^{iq}$ [Eq. (10)] so that both the initial and the first intermediate states must be occupied implying that $i = k = $ HOMO. However, in such a case, both denominators would be off resonance. The contribution from such terms is small and will be neglected, and therefore

$$W_{(rpr)\text{-}MMSh} \sim 0 \text{ (off resonance).} \qquad (A2)$$

A similar procedure can be followed for each of the other terms. In Table I we show the expressions for the Raman scattering amplitudes for all relevant terms. To ensure compact expressions, we have defined the density of occupied states $\mathcal{G}(E) = f(E - E_F)g(E)$ and the density of unoccupied states $\bar{\mathcal{G}}(E) = [1 - f(E - E_F)]g(E)$, where $g(E)$ is the total density of states and $f(E - E_F)$ is the occupation of the states, which can be described by the Fermi-Dirac distribution. It is important to note that some terms such as the rpr-$MSSe$, the rpr-$SMSh$ terms are being neglected due to the fact that they are proportional to the M_{SS}^{ep} term, as discussed in Sec. III A. Also, there are terms which do not contribute to the Raman scattering due to the Pauli exclusion principle. For example, the rrp-$MMSh$ process is proportional to the factor ξ in Eq. (10), and thus involves different occupied initial and intermediate states of the molecule. Since the molecule is assumed to be composed of only one occupied and one unoccupied state, this process is forbidden by the Pauli blocking constraint.

[1] X. Ling, L. Xie, Y. Fang, H. Xu, H. Zhang, J. Kong, M. S. Dresselhaus, J. Zhang, and Z. Liu, Nano Lett. **10**, 553 (2010).

[2] X. Ling and J. Zhang, Small **6**, 2020 (2010).

[3] N. Jung, A. C. Crowther, N. Kim, P. Kim, and L. Brus, ACS Nano **4**, 7005 (2010).

[4] C. Qiu, H. Zhou, H. Yang, M. Chen, Y. Guo, and L. Sun, J. Phys. Chem. C **115**, 10019 (2011).

[5] N. Peimyoo, T. Yu, J. Shang, C. Cong, and H. Yang, Carbon **50**, 201 (2012).

[6] X. Ling, L. G. Moura, M. A. Pimenta, and J. Zhang, J. Phys. Chem. C **116**, 25112 (2012).

[7] L. Xie, X. Ling, Y. Fang, J. Zhang, and Z. Liu, J. Am. Chem. Soc. **131**, 9890 (2009).

[8] S. Huh, J. Park, Y. S. Kim, K. S. Kim, B. H. Hong, and J.-M. Nam, ACS Nano **5**, 9799 (2011).

[9] X. Yu, H. Cai, W. Zhang, X. Li, N. Pan, Y. Luo, X. Wang, and J. G. Hou, ACS Nano **5**, 952 (2011).

[10] C.-Y. Liu, K.-C. Liang, W. Chen, C. hao Tu, C.-P. Liu, and Y. Tzeng, Opt. Express **19**, 17092 (2011).

[11] H. Xu, L. Xie, H. Zhang, and J. Zhang, ACS Nano **5**, 5338 (2011).

[12] H. Xu, Y. Chen, W. Xu, H. Zhang, J. Kong, M. S. Dresselhaus, and J. Zhang, Small **7**, 2945 (2011).

[13] A. Otto, in *Light Scattering in Solids IV*, Topics of Applied Physics Vol. 54, edited by M. Cardona and G. Güntherodt (Springer, Berlin, 1984), pp. 289–418.

[14] A. Otto, I. Mrozek, H. Grabhorn, and W. Akemann, J. Phys.: Condens. Matter **4**, 1143 (1992).

[15] K. Kneipp, Y. Wang, H. Kneipp, L. T. Perelman, I. Itzkan, R. R. Dasari, and M. S. Feld, Phys. Rev. Lett. **78**, 1667 (1997).

[16] A. M. Michaels, M. Nirmal, and L. E. Brus, J. Am. Chem. Soc. **121**, 9932 (1999).

[17] D.-K. Lim, K.-S. Jeon, H. M. Kim, J.-M. Nam, and Y. D. Suh, Nat. Mater. **9**, 60 (2009).

[18] L. Rodriguez-Lorenzo, R. A. Alvarez-Puebla, I. Pastoriza-Santos, S. Mazzucco, O. Stephan, M. Kociak, L. M. Liz-Marzan, and F. J. Garcia de Abajo, J. Am. Chem. Soc. **131**, 4616 (2009).

[19] S. L. Kleinman, E. Ringe, N. Valley, K. L. Wustholz, E. Phillips, K. A. Scheidt, G. C. Schatz, and R. P. Van Duyne, J. Am. Chem. Soc. **133**, 4115 (2011).

[20] M. Stockman, in *Surface-Enhanced Raman Scattering*, Topics in Applied Physics Vol. 103, edited by K. Kneipp, M. Moskovits, and H. Kneipp (Springer, Berlin, 2006), pp. 47–65.

[21] J. R. Lombardi, R. L. Birke, T. Lu, and J. Xu, J. Chem. Phys. **84**, 4174 (1986).

[22] A. C. Albrecht, J. Chem. Phys. **34**, 1476 (1961).

[23] B. N. J. Persson, K. Zhao, and Z. Zhang, Phys. Rev. Lett. **96**, 207401 (2006).

[24] R. M. Martin and L. M. Falicov, *Light Scattering in Solids I*, Topics in Applied Physics Vol. 8 (Springer, Berlin, 1983), pp. 79–145.

[25] D. M. Basko, New J. Phys. **11**, 095011 (2009).

[26] M. Kalbac, A. Reina-Cecco, H. Farhat, J. Kong, L. Kavan, and M. S. Dresselhaus, ACS Nano **4**, 6055 (2010).

[27] C.-F. Chen, C.-H. Park, B. W. Boudouris, J. Horng, B. Geng, C. Girit, A. Zettl, M. F. Crommie, R. A. Segalman *et al.*, Nature (London) **471**, 617 (2011).

[28] K. S. Novoselov, A. K. Geim, S. V. Morozov, D. Jiang, M. I. Katsnelson, I. V. Grigorieva, and S. V. Dubonos, Nature (London) **438**, 197 (2005).